Strong Modification of QD Spontaneous Emission in Slits Young Chul J Phys Chem 09

DATASET · NOVEMBER 2012

READS
76

3 AUTHORS, INCLUDING:

Ragip Pala
California Institute of Technology
20 PUBLICATIONS **708** CITATIONS
SEE PROFILE

Mark L Brongersma
Stanford University
272 PUBLICATIONS **12,145** CITATIONS
SEE PROFILE

Strong Modification of Quantum Dot Spontaneous Emission via Gap Plasmon Coupling in Metal Nanoslits†

Young Chul Jun, Ragip Pala, and Mark L. Brongersma*

Geballe Laboratory for Advanced Materials, Stanford, California 94305

Received: August 28, 2009; Revised Manuscript Received: October 10, 2009

A metal−dielectric−metal (MDM) waveguide with a nanoscale gap supports highly confined surface plasmon−polariton modes, termed gap plasmons. The spontaneous emission of an emitter placed in such a metal nanogap is expected to be strongly modified due to coupling to gap plasmons. We investigate the light emission properties of semiconductor quantum dots (QD) in a metal nanoslit, which is a truncated MDM waveguide. More specifically, we measure both the lifetime and the state of polarization of the out-coupled QD emission from a metal nanoslit. We observe clear lifetime and polarization changes of QD emission. As the slit width gets smaller, the QD exciton lifetime gradually decreases, and its emission becomes polarized normal to the slit, as expected for gap plasmon coupled light emission. We also find that the polarization of the collected QD emission is flipped (i.e., becomes parallel to a slit) when the excited emitters are located just outside the slit. We have conducted dipole emission calculations in metal nanoslits, and these explain the experimentally observed lifetime and polarization changes well. These findings may have novel applications in nanoscale optical sources, sensors, and active devices.

Introduction

Studies of spontaneous emission (SE) in compact, solid-state device structures have been of interest for both fundamental science studies and practical device applications.[1] Recently, metallic structures (such as metal films,[2,3] nanoparticles,[4,5] and nanowires[6,7]) have attracted significant attention for their ability to enhance the SE of light emitters. Coupling of emitters to subwavelength surface plasmon−polariton (SPP) modes enables substantial SE enhancement with relatively simple geometries. A metal−dielectric−metal (MDM) waveguide, consisting of a thin (a few tens of nanometers) dielectric layer sandwiched between two metal films, provides particularly exciting opportunities for radiative decay engineering. For sufficiently small spacings, it supports a single, highly confined, transverse, magnetic (TM) SPP mode, termed a gap plasmon.[8,9] Recent theoretical studies pointed out that the SE in such a metal nanogap is strongly enhanced due to gap plasmon excitation.[10,11] In contrast to metal nanoholes,[12,13] the metal-to-metal (i.e., gap) spacing in a MDM structure can be reduced without waveguide mode cutoff, enabling extremely high field confinement and large SE enhancement. Additionally, MDM structures can be integrated with other electrical and optical components on the same chip. This geometry thus holds great promise for implementing highly integrated nanoscale optical sources and active devices as well as novel coherent nearfield sources.[14,15]

Here, we investigate the light emission properties of semiconductor quantum dots (QD) in a metal nanoslit (Figure 1a, b), which is a truncated MDM structure that provides a natural pathway of light coupling into and out of a metal nanogap. In room temperature photoluminescence measurements, we observe clear lifetime and polarization changes of QD emission with slit dimensions and explain these changes by modification of the coupling to the SPP modes supported by the nanoslits. As the slit width gets smaller, the QD exciton lifetime gradually decreases, and its emission becomes polarized normal to the slit, as expected for gap plasmon coupling in metal nanoslits. We also find that the polarization of the collected QD emission becomes parallel to a slit when excited emitters are located just outside the slit. The polarization-dependent light transmission in a metal nanoslit (Figure 1c, d) enables this unique polariza-

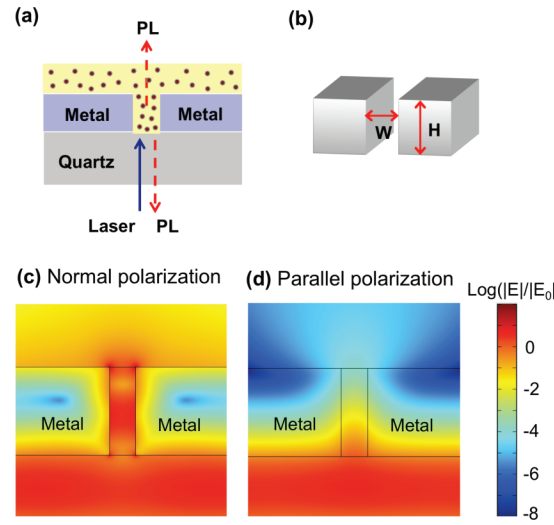

Figure 1. (a) Schematic of the experiment configuration. The pump laser illuminates the sample from the transparent quartz substrate, and quantum dot photoluminescence is collected from either the top or bottom. CdSe/ZnS QDs are mixed with PMMA and spin-coated on silver nanoslits. The pump laser wavelength is 481 nm, and the QD emission is centered at 610 nm. (b) Geometry of the sample. The metal film thickness (H) was fixed as 200 nm, and the slit width (W) was varied. (c, d) Numerical simulation of light transmission through a silver nanoslit ($W = 60$ nm, $H = 200$ nm). A plane wave is incident from the bottom, and its electric field magnitude is plotted (log scale). The electric field of the incident light is either (c) normal to the slit or (d) parallel to the slit. Normally polarized light passes through a slit and has a much stronger field on the top metal surface than that of parallel polarization, which is rapidly attenuated inside the slit.

† Part of the "Martin Moskovits Festschrift".

* Corresponding author. E-mail: brongersma@stanford.edu.

10.1021/jp9083376
Published on Web 11/10/2009

tion-dependent excitation and collection of QD emission. We have conducted dipole emission calculations in metal nanoslits, and these explain the experimental observations well. The enhanced SE rate can result in the enhancement of an emitter's quantum efficiency and response time, and this may have applications in nanoscale optical sources and sensors. Because a nanoslit is also ideal for applying an electric field across the slit and isolating single emitters, slits may also be useful for electro-optic active devices, single QD spectroscopy, and a variety of quantum optics experiments.

Methods

A 200 nm layer of silver (Ag) was evaporated on transparent quartz, together with a 5 nm adhesion layer of chromium. Nanoslits were milled by a focused ion beam (FIB). The slit widths were measured with a scanning electron microscope after FIB milling. First, the slits were covered with a 10 nm aluminum oxide buffer layer with atomic layer deposition (ALD). This layer serves to limit the strong coupling to lossy waves, which is an undesired nonradiative decay channel.[16−18] Next, a thin layer (∼15 nm) of poly methylmethacrylate (PMMA) that was mixed with colloidal CdSe/ZnS QDs (from Evident Technologies) was spin-coated on top. From the QD solution density and PMMA concentration, we get the estimated mean spacing between QDs to be ∼20 nm. After dropcasting the PMMA solution on the substrate, we allowed about 1 min for the QDs to enter the slits through the action of capillary forces before spinning. The resulting sample geometry with some QDs inside the slit and on top of the metal film surface is shown in Figure 1a and b.

Figure 1c and d show the numerically simulated field profile inside a silver nanoslit for normal and parallel polarization incidence of light. For parallel polarization incidence, light attenuates mainly inside the slit. However, normally polarized light passes through a slit and has several orders of magnitude stronger field above the metal slit than that of parallel polarization. Through a choice of the polarization direction of the pump, we can thus choose to selectively excite QDs inside the slit (parallel polarization) or all of the dots inside and on top of the metal surface (normal polarization).

For time-resolved photoluminescence (PL) measurements, QDs were excited with a picosecond pulsed diode laser at 481 nm from a transparent substrate, and QD emission (centered at 610 nm) was collected either from the top or from the bottom (Figure 1a). The pump laser power (measured before a microscope objective) was <1 μW. The PL lifetimes of QDs were measured using a single photon avalanche detector (Micro Photon Devices) and a time-correlated single photon counting system (PicoQuant).

For the theoretical modeling of QD emission, we have performed dipole emission calculations. The SE rate can be obtained by calculating the emitted power from a classical electric dipole source. First, we consider the total SE enhancement of a dipole source in planar MDM waveguides, which can be calculated from an analytical formulation.[16−19] Calculation of the emitted power from a dipole source is equivalent to obtaining the work done on the dipole by its own reflected field. For a planar structure, the reflected field can be obtained through a plane-wave decomposition and successive applications of the Fresnel reflection coefficients. In our previous work, we have theoretically analyzed dipole emission in MDM structures and found that it is strongly enhanced due to gap plasmon excitations.[11]

In a second step, we consider metal films with finite thicknesses and perform 3D finite-difference time domain (FDTD) simulations. The SE enhancement can be obtained by measuring the total outgoing flux from an electric dipole source and normalizing it by the flux in a background dielectric medium:[20] $\langle\gamma\rangle/\langle\gamma_0\rangle = \langle P\rangle/\langle P_0\rangle$, where $\langle P\rangle$ and $\langle P_0\rangle$ are the time-averaged outgoing flux from a dipole with and without metal structures. This numerical technique has been applied successfully to other metal nanostructures, as well.[21,22]

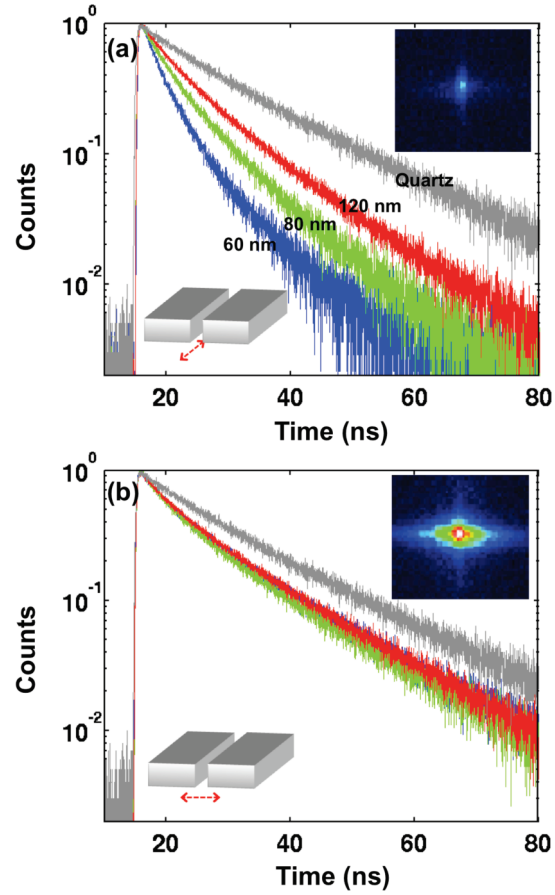

Figure 2. Normalized decay tail of CdSe/ZnS QD emission from silver nanoslits for (a) parallel laser pumping and (b) normal laser pumping (blue, $W = 60$ nm; green, $W = 80$ nm; red, $W = 120$ nm; gray, on quartz). Inset: PL images taken from above the sample.

Results and Discussion

Top Collection of QD Emission. We first measured PL decay curves (Figure 2) and polarization changes (Figure 3) in Ag slits for two pump laser polarizations. When the pump laser is polarized parallel to the slit, we observe clear changes in the decay curve (Figure 2a) and the polarization (Figure 3b). As the slit gets narrower, the QD lifetime gradually decreases and the QD PL becomes more polarized normal to the slit, as expected for gap plasmon coupling of QD emission. CdSe QDs are known to have a 2D degenerate emission dipole moment and emit light into the plane normal to the *c*-axis of the nanocrystal.[23] In the ensemble of QDs, this dark axis is randomly oriented, so light emission from the QD ensemble is unpolarized. Therefore, the fact that we have strongly polarized light from a metal nanoslit implies that the QD emission is coupled to the optical mode supported by the metal nanoslit.[24] We observed similar lifetime and polarization changes of the QD emission in gold and aluminum nanoslits, as well (not shown). By fitting decay curves in Figure 2a to a stretched exponential,[25] we obtain the QD exciton lifetimes of 3.6 (for $W = 60$ nm), 5.6 (for $W =$

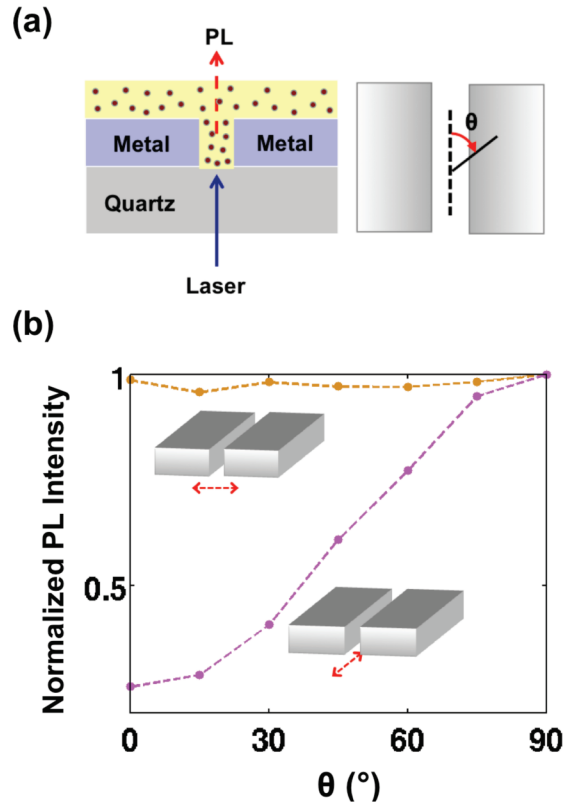

Figure 3. (a) Schematic of the top PL collection and the definition of PL polarization angle. $\theta = 0°$ and $\theta = 90°$ correspond to parallel and normal to the slit, respectively. (b) Normalized PL intensity for two pump laser polarizations as a function of polarization angle for a $W =$ 60 nm slit. PL is strongly polarized normal to the slit for parallel pumping, whereas it is almost unpolarized for normal pumping.

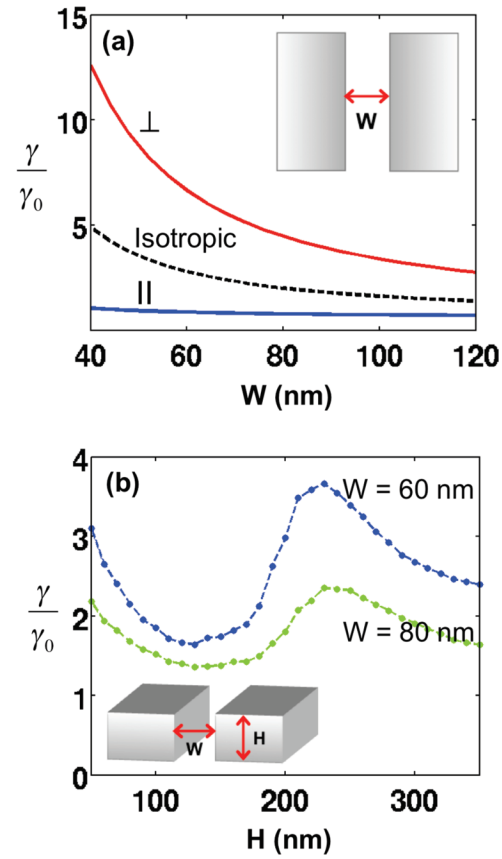

Figure 4. Calculated normalized decay rates for (a) a planar MDM layer as a function of metal gap width (W) and (b) a thin metal film as a function of metal thickness (H). Metal is silver, and dielectric has $\varepsilon = 2.25$. $\lambda_0 = 610$ nm.

80 nm), 7.5 (for $W = 120$ nm), and 14.3 ns (on bare quartz). However, when the pump polarization is normal to the slit, we essentially do not observe lifetime and polarization changes with slit width (Figures 2b and 3b). We also do not see an observable decay curve change with laser power. This excludes pump-power-dependent processes in our system around the laser power we used.

The observed changes in the PL properties for a parallel polarization of the illumination beam are representative of changes in the coupling of QDs inside the slit to gap plasmons. According to Figure 1d, the QDs inside the slit are selectively excited under these pumping conditions. The absence of strong changes in the PL properties for a normally polarized pump is explained by the fact that QDs on top of the metal surface are excited, as well; their PL properties are only weakly dependent on the slit properties. The validity of this statement is further confirmed by PL images of the slit region, which show drastic differences between the two pump laser polarizations. For normal pump polarization, the PL spot (inset in Figure 2b) is large and covers a broad metal area. In contrast, with the parallel pumping, we see that the PL mostly comes from the slit (inset in Figure 2a).

To compare the experimental observations with a theoretical model, we have investigated the dependence of the SE rate of a dipolar emitter on the slit width. We first considered a planar MDM waveguide, which can be studied from an analytical formulation.[16,17] Figure 4a shows the calculated SE enhancements for dipoles oscillating normal and parallel to metal surfaces as a function of gap width. We assume a 50% quantum efficiency (QE) of the dipole source. The decay rates are spatially averaged inside the gap, excluding the 10-nm-thick ALD oxide buffer region on each metal surface. As the gap width decreases, the normal dipole decay rates rapidly increase due to the gap plasmon excitation, while the parallel dipole decay rate does not change noticeably. For a more detailed discussion, see, for example, Figures 2 and 3 in ref 11. The highly directional field profile of gap plasmons inside a metal gap causes this drastic difference for these two dipole orientations, and the out-coupled light from gap plasmons is thus also expected to be polarized normal to a metal gap, as we observe experimentally. The isotropically averaged decay rates ($\gamma_{iso} = \gamma_{\perp}/3 + 2\gamma_{\parallel}/3$) are also plotted. We obtain enhancement factors of three and two for the $W = 60$ and 80 nm slits, respectively.

To investigate the effect of the finite metal film thickness, we have conducted dipole emission calculations with 3D-FDTD simulations. Figure 4b shows the isotropically averaged decay rate ($\gamma_{iso} = [\gamma_x + \gamma_y + \gamma_z]/3$) of a dipole source as a function of metal film thickness. A dipole is located in the center of the slit, and we assume a 50% quantum efficiency for a dipole source. Reflections from slit terminations are known to cause a Fabry−Perot resonance when the slit length is close to half the gap plasmon wavelength,[26,27] and this also results in a peak in the SE rate enhancement. In addition, the SE rate is also strongly enhanced in a very thin metal layer limit due to enhanced excitation of 1-dimensional slot waveguide modes.[11] This thickness dependence suggests that we can control the QD light emission direction as well as its SE rate in a metal nanoslit, via simply optimizing metal film thicknesses. The experimentally observed decay rate enhancements are reasonably close to the values in Figure 4a and b, but we find that the experimental

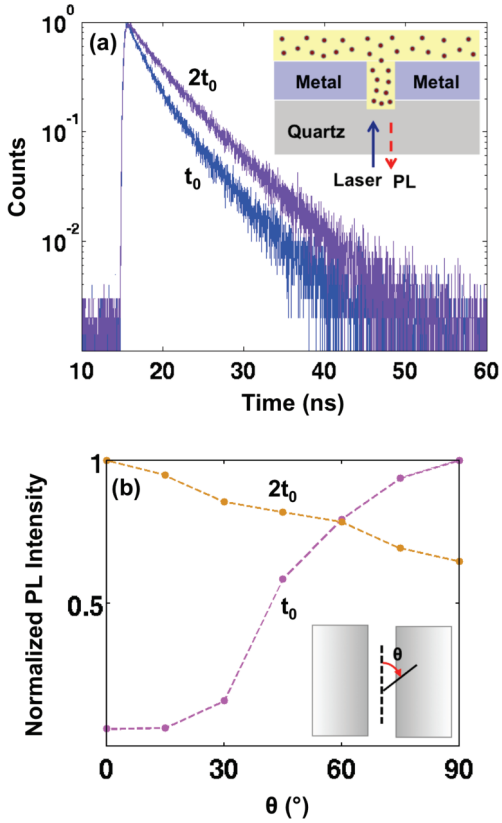

Figure 5. (a) Normalized decay tail of QD emission collected from the substrate. The inset is the schematic of the bottom PL collection. (b) Normalized PL intensity as a function of polarization angle for a slit terminating on the quartz substrate and for an overmilled slit generated by FIB milling for twice as long. The angles $\theta = 0°$ and $\theta = 90°$ correspond to parallel and normal to the slit, respectively. In the overmilled slit, the polarization of collected QD emission is flipped (i.e., parallel to the slit).

values are slightly larger. The difference can be due to the larger QD QE[28−30] or smaller averaged slit widths (due to the sidewall slope) than what we assumed in the calculations. The distribution of QDs inside the slit may not be perfectly uniform either,[31] in contrast to what was assumed in our simulations.

Bottom Collection of QD Emission. The QD emission collected through the transparent quartz substrate also exhibits clear lifetime and polarization changes with slit width. However, we observe further changes in the emission properties for different FIB milling depths. Figure 5 compares the lifetime and polarization of the QD emission collected from the substrate for slits with two different milling times. The pump laser was polarized parallel to the slit. In a slit that was milled down to the metal/quarts interface, the PL is again polarized normal to the slit. However, in an overmilled slit (twice the milling time), the lifetime is longer, and the PL polarization becomes parallel to the slit. Because there were no observable changes in slit widths with this milling time variation, the QDs in the overmilled portion into a quartz substrate must have emission properties different from those inside the slit.

The "*polarization flip*" that occurs with increased milling depth is surprising at first sight, but numerical simulations retrieve this feature. We have investigated it with 3D-FDTD simulations. We move a dipole source gradually across the slit boundary and measure the outgoing flux into the substrate (Figure 6a). By looking at the flux ratio from normal and parallel dipoles, we can see how the polarization state of the collected light changes with dipole position. Figure 6b shows the plot of

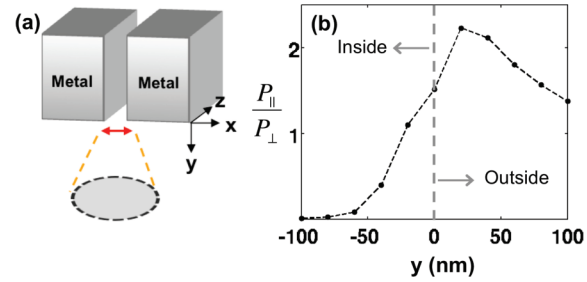

Figure 6. (a) Schematic of dipole emission calculation with 3D-FDTD simulations. A gray circle indicates the flux collection area. Its size was decided by considering a numerical aperture (i.e., collection angle) of the microscope objective used in our experiment. (b) Flux ratio between parallel (z-) and normal (x-) dipoles as a function of a dipole position. The dipole positions $y < 0$, $y > 0$, $y = -100$ nm, and $y = 0$ nm correspond to the inside, outside, center, and the edge of the metal slit, respectively. $W = 60$ nm and $H = 200$ nm.

this flux ratio. We see that as a dipole crosses the slit boundary, the flux ratio changes rapidly, which explains the experimentally observed polarization flip. When a dipole is close to the center of the slit, the ratio is much smaller than 1; that is, the collected light is strongly polarized normal to the slit. As the dipole crosses the slit boundary, the ratio becomes larger than 1; that is, the collected light is polarized parallel to the slit. As the dipole moves away from the metal slit, its total decay rate drops quickly due to the reduced slit mode coupling. However, the nanoslit still affects the direction of the light emission. When a dipole is positioned just outside a slit, its parallel dipole emission is mainly back-reflected into the quartz substrate, whereas its normal dipole emission can still efficiently couple into the slit and out the other side. This is consistent with the strong polarization dependence of light transmission through a metal nanoslit, as shown in Figure 1c, d. The emission direction of a normal dipole also has a larger solid angle toward a slit and thus favors the slit coupling. This polarization property of light emission in metal nanoslits may find novel applications in single molecule analysis or biosensors, utilizing metal nanoapertures.[12,13,32]

Conclusion

In conclusion, we have investigated the light emission properties of semiconductor QDs in metal nanoslits. We observe clear lifetime and polarization changes in the QD emission with slit width due to gap plasmon excitation in metal nanoslits. We also find that the collected QD emission polarization can be either normal or parallel to a slit, depending on the emitter position. These findings may have novel applications in implementing nanoscale optical sources, sensors, and active devices. The out-coupling of gap plasmons to far-field light can be increased with side gratings, and they can further help improve the directivity of the out-coupled light.[33] A nanoslit is also ideal for isolating single QDs and supports a natural way of light coupling into and out-of a metal nanogap. Therefore, we expect it can find useful applications in single QD spectroscopy and various quantum optics experiments as well.[6,34,35]

Acknowledgment. The authors thank J. Liu for help in the preparation of the manuscript. This work was funded by the DOE (Grant No. F49550-04-10437). Y.C.J. acknowledges the support of a Samsung scholarship.

References and Notes

(1) Burstein, E., Weisbuch, C., Eds. *Confined electrons and photons*; Plenum Press: New York, NY, 1995.

(2) Neogi, A.; Lee, C.-W.; Everitt, H. O.; Kuroda, T.; Tackeuchi, A.; Yablonovitch, E. *Phys. Rev. B* **2002**, *66*, 153305.
(3) Okamoto, K.; Niki, I.; Shvartser, A.; Narukawa, Y.; Mukai, T.; Scherer, A. *Nat. Mater.* **2004**, *3*, 601.
(4) Anger, P.; Bharadwaj, P.; Novotny, L. *Phys. Rev. Lett.* **2006**, *96*, 113002.
(5) Kühn, S.; Håkanson, U.; Rogobete, L.; Sandoghdar, V. *Phys. Rev. Lett.* **2006**, *97*, 017402.
(6) Akimov, A. V.; Mukherjee, A.; Yu, C. L.; Chang, D. E.; Zibrov, A. S.; Hemmer, P. R.; Park, H.; Lukin, M. D. *Nature* **2007**, *450*, 402.
(7) Fedutik, Y.; Temnov, V. V.; Schöps, O.; Woggon, U.; Artemyev, M. V. *Phys. Rev. Lett.* **2007**, *99*, 136802.
(8) Zia, R.; Selker, M. D.; Catrysse, P. B.; Brongersma, M. L. *J. Opt. Soc. Am. A* **2004**, *21*, 2442.
(9) Dionne, J. A.; Lezec, H. J.; Atwater, H. A. *Nano Lett.* **2006**, *6*, 1928.
(10) Maier, S. A. *Opt. Express* **2006**, *14*, 1957.
(11) Jun, Y. C.; Kekatpure, R. D.; White, J. S.; Brongersma, M. L. *Phys. Rev. B* **2008**, *78*, 153111.
(12) Levene, M. J.; Korlach, J.; Turner, S. W.; Foquet, M.; Craighead, H. G.; Webb, W. W. *Science* **2003**, *299*, 682.
(13) Wenger, J.; Gerard, D.; Dintinger, J.; Mahboub, O.; Bonod, N.; Popov, E.; Ebbesen, T. W.; Rigneault, H. *Opt. Express* **2008**, *16*, 3008.
(14) Bergman, D. J.; Stockman, M. I. *Phys. Rev. Lett.* **2003**, *90*, 027402.
(15) Stockman, M. I. *Nat. Photon.* **2008**, *2*, 327.
(16) Chance, R.; Prock, A.; Silby, R. *Adv. Chem. Phys.* **1978**, *37*, 1.
(17) Ford, G. W.; Weber, W. H. *Phys. Rep.* **1984**, *113*, 195.
(18) Barnes, W. L. *J. Mod. Opt.* **1998**, *45*, 661.
(19) Novotny, L.; Hecht, B., *Principles of Nano-Optics*; Cambridge University Press: Cambridge, UK, 2006; pp 277−283.
(20) Xu, Y.; Lee, R. K.; Yariv, A. *Phys. Rev. A* **2000**, *61*, 033807.
(21) Mohammadi, A.; Sandoghdar, V.; Agio, M. *New J. Phys.* **2008**, *10*, 105015.
(22) Liu, M.; Lee, T.-W.; Gray, S. K.; Guyot-Sionnest, P.; Pelton, M. *Phys. Rev. Lett.* **2009**, *102*, 107401.
(23) Chung, I.; Shimizu, K. T.; Bawendi, M. G. *Proc. Natl. Acad. Sci. U.S.A.* **2003**, *100*, 405.
(24) Mertens, H.; Biteen, J. S.; Atwater, H. A.; Polman, A. *Nano Lett.* **2006**, *6*, 2622.
(25) Lindsey, C. P.; Patterson, G. D. *J. Chem. Phys.* **1980**, *73*, 3348.
(26) White, J. S.; Veronis, G.; Yu, Z.; Barnard, E. S.; Chandran, A.; Fan, S.; Brongersma, M. L. *Opt. Lett.* **2009**, *34*, 686.
(27) Kuttge, M.; Garcia de Abajo, F. J.; Polman, A. *Opt. Express* **2009**, *17*, 10385.
(28) Fisher, B. R.; Eisler, H.-J.; Stott, N. E.; Bawendi, M. G. *J. Phys. Chem. B* **2004**, *108*, 143.
(29) Brokmann, X.; Coolen, L.; Dahan, M.; Hermier, J. P. *Phys. Rev. Lett.* **2004**, *93*, 107403.
(30) Leistikow, M. D.; Johansen, J.; Kettelarij, A. J.; Lodahl, P.; Vos, W. L. *Phys. Rev. B* **2009**, *79*, 045301.
(31) Brongersma, M. L.; Polman, A.; Min, K. S.; Atwater, H. A. *J. Appl. Phys.* **1999**, *86*, 759.
(32) Eftekhari, F.; Escobedo, C.; Ferreira, J.; Duan, X.; Girotto, E. M.; Brolo, A. G.; Gordon, R.; Sinton, D. *Anal. Chem.* **2009**, *81*, 4308.
(33) Lezec, H. J.; Degiron, A.; Devaux, E.; Linke, R. A.; Martin-Moreno, L.; Garcia-Vidal, F. J.; Ebbesen, T. W. *Science* **2002**, *297*, 820.
(34) Chang, D. E.; Sorensen, A. S.; Hemmer, P. R.; Lukin, M. D. *Phys. Rev. Lett.* **2006**, *97*, 053002.
(35) Chang, D. E.; Lukin, M. D. *Nat. Phys.* **2007**, *3*, 807.

JP9083376